applied sciences

MDPI

Review

Review of Fast Computation Methods for Finite-State Predictive Control of Multi-Phase Drives

Esteban Marsal [1,†], Manuel R. Arahal [1,*,†], Manuel G. Satué [1] and Manuel Perales [2]

[1] Systems Engineering and Automation Department, Escuela Técnica Superior de Ingeniería, University of Seville, Camino de los Descubrimientos s/n, 41092 Seville, Spain; lmarsal@us.es (E.M.); mgarrido16@us.es (M.G.S.)
[2] Electronic Engineering Department, Escuela Técnica Superior de Ingeniería, University of Seville, Camino de los Descubrimientos s/n, 41092 Seville, Spain; mperales@us.es
* Correspondence: arahal@us.es
† These authors contributed equally to this work.

Abstract: Optimizing the cost function in predictive control of multi-phase drives is computationally intensive. This poses a challenge since the required sampling period for drives falls within the microsecond range. Numerous methods have been proposed in the literature to address this computational demand. This paper reviews recent proposals for multi-phase drives of various kinds. A structured classification of the proposals is provided. Furthermore, an integrated framework is employed to cohesively present and connect previously unrelated methods. Key elements such as Allowed Control Set, inter-sample modulation, and weighting factor use are identified. New developments in multi-vector and single-vector approaches are discussed. Practical limitations for each approach are also considered.

Keywords: computational reduction; fast computation; finite state model predictive control; induction motor; multi-phase drives; variable speed drives

check for updates

Citation: Marsal, E.; Arahal, M.R.; Satué, M.G.; Perales, M. Review of Fast Computation Methods for Finite-State Predictive Control of Multi-Phase Drives. *Appl. Sci.* **2024**, *14*, 11774. https://doi.org/10.3390/app142411774

Academic Editor: Alessandro Lo Schiavo

Received: 22 November 2024
Revised: 12 December 2024
Accepted: 15 December 2024
Published: 17 December 2024

Copyright: © 2024 by the authors. Licensee MDPI, Basel, Switzerland. This article is an open access article distributed under the terms and conditions of the Creative Commons Attribution (CC BY) license (https://creativecommons.org/licenses/by/4.0/).

1. Introduction

Model Predictive Control (MPC) was initially introduced in the 1970s to handle complex dynamics, such as those found in chemical processes [1]. Its early applications were primarily for slow processes due to the high computational demand of MPC compared to PID control. The demand is largely due to the optimization stage. In said stage, a cost function (CF) assigns penalties to anticipated deviations of variables from their set points, as well as to additional terms (e.g., control effort). For linear systems with specific assumptions, this optimization process can be relatively straightforward. However, for general non-linear dynamics, the optimization becomes more complex, requiring significant computational time [2].

In the 1980s, as more advanced computing devices became available, the MPC method was proposed for controlling drives [3]. Typical control configurations for AC drives involve an inner loop for current regulation and an outer loop for rotor flux and speed control, with the predictive controller potentially handling both roles. The more challenging task is replacing the inner loop, as it involves a faster dynamics response [4].

A particular predictive setup is accomplished by executing direct digital control of the Voltage Source Inverter (VSI) [5]. In this arrangement, the VSI state is directly set by the MPC, eliminating intermediate modulation stages. This configuration is known as Finite-State MPC (FSMPC) or Finite-Control-Set MPC (FCSMPC) [6]. Here, the VSI state effectively becomes the control signal, and the primary term of the cost function can be specified in terms of either stator currents or electric torque and rotor flux. The first option is of interest in this context, as it has been favored in multi-phase research.

The FSMPC approach has been the subject of research for the control of drives of different kinds, including induction, permanent magnet, reluctance, and other systems. In this review, the focus is put on MPS regardless of the kind of machine. It is worth recalling that electric multi-phase systems (MPS) offer certain benefits over conventional three-phase systems. In drives, multi-phase motors exhibit reduced torque oscillations, lower DC-link harmonics, enhanced fault tolerance, and improved phase power distribution [7]. Owing to these advantages, multi-phase drives have attracted research interest for applications like renewable energy systems, vehicle traction, and ship propulsion [8].

In MPS, the collection of phases is simplified by using the Vector Space Decomposition (VSD) method [9]. This projection maps phase quantities onto multiple planes. One plane, referred to as the α-β plane, is responsible for torque production, while others (x-y planes) contribute to losses without generating torque. Finally, planes such as $z_1 - z_2$ might be absent in most configurations since homopolar currents typically do not flow. Through this decomposition, the FSMPC cost function can be defined in terms of the α-β and (termed x-y) currents as primary objectives [10].

One significant reason for the recent expansion of MPC applications is the adaptability it provides. This adaptability arises from two main aspects. First, the use of a model allows MPC to be applied in challenging scenarios. These scenarios include multi-variable cases, existence of disturbances, delays, and non-linear behaviors [2]. The second factor is the use of a cost function to guide control action selection. The cost function can incorporate numerous terms and constraints, making it possible to address multiple objectives. In the case of FSMPC for MPS, the primary objectives are α-β tracking and x-y minimization. Additional objectives, such as penalizing VSI switching frequency, are also possible [10].

However, the optimization of the CF on a sample-by-sample basis requires considerable computational time. This poses a challenge for electrical drives, as the sampling period for stator current control needs to be in the microsecond range. Longer sampling intervals lead to less effective modulation of stator voltages and a reduced bandwidth [11]. Please note that until recently, switching frequency was a major concern for some FSMPC proposals. This concern is progressively being reduced thanks to the introduction of modern power devices based on SiC [12,13] and GaN technologies [14,15].

Various methods have been proposed in the literature to address this issue. This paper examines those approaches relevant to MPS, offering a structured classification of the different solutions. Additionally, an integrated framework is used to present previously unrelated methods.

The following section introduces the FSMPC framework for MPS, focusing on stator current control. Section 3 provides a classification of previous approaches based on factors that influence computational load. A critical assessment is then presented in Section 4.

2. MPC for Current Control of MPS

In this section, the basic elements of FSMPC are reviewed. In the description that follows, a five-phase induction motor is used as a reference and to provide a concrete example. As discussed in the Introduction, MPC concepts have been widely applied in the field of variable-speed drives, with predictive stator current control being one of the most relevant approaches for MPS. The relevant components of this control scheme are depicted in Figure 1 and are detailed below. The reference example is based on the work presented in [16].

2.1. Drive Control

FSMPC for variable-speed drives builds upon the Indirect Field-Oriented Control (IFOC) scheme [17]. This approach incorporates an outer feedback loop for speed regulation and an inner feedback loop dedicated to stator current control, as shown in Figure 1.

For MPS, phase stator currents are transformed using the Clarke projection into the α-β and x-y planes. This transformation enables the decoupling of control variables, simplifying the control strategy. According to the IFOC approach, the torque-generating currents should track a reference value set by the torque/speed control loop. The x-y current references

are maintained at zero to minimize energy losses. In this manner, rotor flux and torque are regulated independently. The rotor flux target is given by i_d^*, while i_q^* serves as the reference for electrical torque. These references are projected onto the α-β plane via the Park transformation, resulting in a reference stator current in the α-β space as $I_{s\alpha-\beta}^* = D\left(i_d^*, i_q^*\right)^\intercal$, where matrix D is defined as

$$D = \begin{pmatrix} \cos\,\theta_a & \sin\,\theta_a \\ -\sin\,\theta_a & \cos\,\theta_a \end{pmatrix}. \tag{1}$$

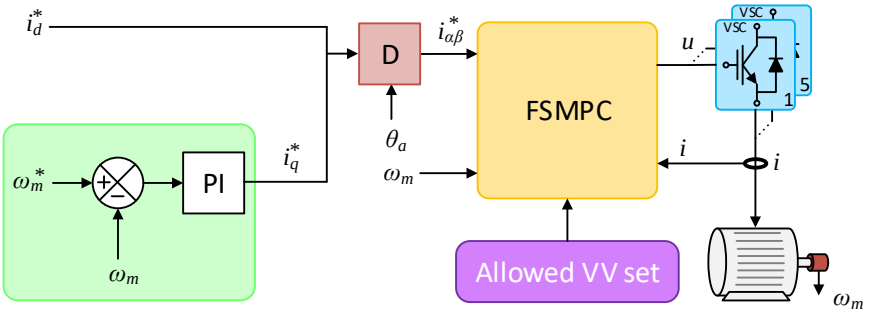


Figure 1. Diagram of FSMPC for a five-phase IM.

The rotor flux position θ_a is estimated as $\theta_a = \int \omega_e\, dt$, where $\omega_e = \omega_{sl} + P\omega$, with P being the number of pairs of poles of the IM and ω_{sl} the slip. This last quantity is related to rotor flux linkage (ψ_r) as $\omega_{sl} = i_{qs}/(\tau_r \psi_r / L_m)$, where τ_r is the rotor time constant and L_m the mutual inductance. This expression can be simplified so that direct stator current is used instead of rotor flux, as it is the usual approach for IFOC. With this, one obtains $\omega_{sl} = i_{qs}/(i_{ds}\hat{\tau}_r)$, where $\hat{\tau}_r$ is an estimation of the rotor time constant $\tau_r = L_r/R_r$, with L_r being the rotor inductance and R_r the rotor resistance, respectively. As a result, the set point for stator current tracking $I_s^*(k)$ has an amplitude given by $I_s^* = \sqrt{i_d^{*2} + i_q^{*2}}$. Finally, the α-β references can be expressed as

$$I_{s\alpha}^*(t) = I_s^* \sin(\omega_e t), \quad I_{s\beta}^*(t) = I_s^* \cos(\omega_e t), \quad I_{sx}^*(t) = 0, \quad I_{sy}^*(t) = 0. \tag{2}$$

At this point, the role of FSMPC is the generation of stator currents by issuing voltages through a VSI. This process is influenced by the specific VSI configuration and the number of phases, as described below.

2.2. VSI States and Voltages

In a power-converter-supplied drive, the phase voltages are determined by the VSI state. This state can be represented as a vector $u = (K_a, K_b, \cdots, K_e)^\top$, where the values K_h indicate the state of the corresponding VSI switch for phase h. For a five-phase VSI, there are 32 possible configurations, ranging from $u_0 = (0,0,0,0,0)^\intercal$ to $u_{31} = (1,1,1,1,1)^\intercal$. Each configuration results in a specific set of phase voltages. The stator voltages corresponding to each VSI state can be expressed as $V(k) = V_{DC}TMu(k)$, where V_{DC} is the voltage supplied to the DC-link, and T and M are derived from the VSI structure [18].

The stator voltages can be mapped to the α-β and x-y subspaces using the Clarke transformation. The resulting voltages in the $\alpha\beta xy$ coordinate system are referred to as voltage vectors (VVs). Figure 2 illustrates the distribution of VVs for a five-phase VSI.

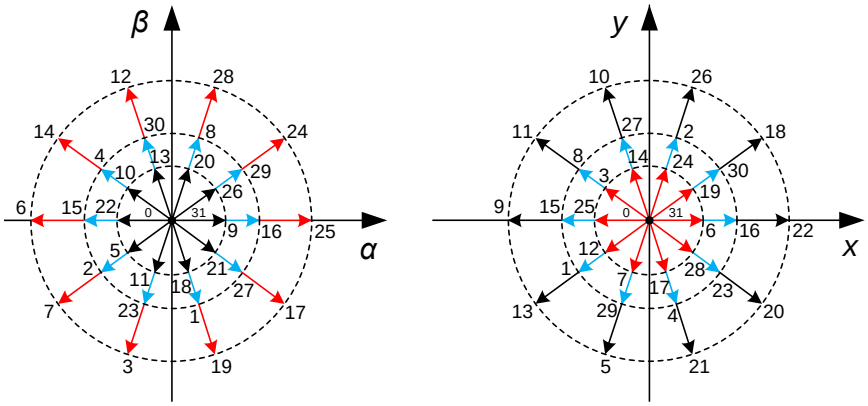


Figure 2. Voltage vectors for a five-phase VSI.

2.3. Basic VV and Virtual VV

As discussed in the previous sections, each VSI configuration generates a specific voltage in the α-β-x-y axes. This voltage is referred to as the basic Voltage Vector (VV). It is useful to describe the distribution of these basic VVs according to their magnitude in the α-β subspace:

1. Large VV (LVV): These are VVs that have the largest magnitude in the α-β subspace, as shown in Figure 2.
2. Medium VV (MVV): These VVs are placed in the second largest corona.
3. Small VV (SVV): These VVs are placed in the smallest corona.
4. Null Voltage (ZVV): This refers to the VVs in the origin.

FSMPC can select any of these basic VVs to be applied at each sampling period. Approaches that follow this strategy are known as single-vector FSMPC. However, it is also possible to release a sequence of basic VVs during a single sampling period. This results in a form of explicit inter-sample modulation. The average voltage generated over the sampling period can be interpreted as a Virtual VV or Synthesized VV [19].

While there are several variants of the Virtual Voltage Vector (VVV) technique, it is particularly useful to focus on VVV for x-y elimination. In this method, VVs are chosen such that their average x-y excitation is zero. For example, a Large VV applied during a subperiod T^L followed by a Medium VV during T^M is selected. The time durations T^L and T^M are chosen so that they add up to the sampling period $T^L + T^M = T_s$. Additionally, the average voltage in the α-β subspace over the sampling period is set to zero, $\overline{V}_{xy} = 0$. This cancellation is achieved by pairing an LVV with an MVV positioned in the opposite part of the x-y subspace.

2.4. Predictive Model

In standard FSMPC, the control action is defined by the state of the VSI, denoted as u. In multi-vector approaches, the control action consists of a sequence of different VSI configurations applied during a sample period. For example, in the case of Virtual Voltage Vector (VVV) techniques, each control action corresponds to a specific VVV. For the following discussion, it may be simpler to focus on the single-vector approach.

FSMPC employs a predictive model to relate predicted stator currents to potential control actions. This model is typically represented by a set of discrete-time state-space equations, as $\hat{i}(k+1) = (C(\omega) + G)i(k) + BV(k)$, where i contains the α, β, x, and y stator currents, $\hat{i}$ is the prediction of i, and ω is the angular speed. Matrices C and B are

obtained from first principles applying time discretization with sampling time T_s. This gives $C = (I + A_c T_s)$ and $B = T_s B_c$, where

$$A_c = \begin{pmatrix} a_2 & -a_4 & 0 & 0 \\ a_4 & a_2 & 0 & 0 \\ 0 & 0 & a_3 & 0 \\ 0 & 0 & 0 & a_3 \end{pmatrix}, B_c = \begin{pmatrix} c_2 & 0 & 0 & 0 \\ 0 & c_2 & 0 & 0 \\ 0 & 0 & c_3 & 0 \\ 0 & 0 & 0 & c_3 \end{pmatrix} \tag{3}$$

In the previous expressions, the coefficients used are $a_2 = -R_s c_2$, $a_3 = -R_s c_3$, $a_4 = -L_M c_4 \omega_r$, which depend on machine parameters such as $c_1 = L_s L_r - L_M^2$, $c_2 = L_r / c_1$, $c_3 = 1/L_{ls}$, $c_4 = L_M / c_1$. Furthermore, term G represents the effect of the rotor currents, which are typically unmeasured. Various methods for estimating these currents have been proposed to improve predictions [20,21].

Using the above expressions, the two-step-ahead prediction of the stator currents can be expressed as

$$\hat{i}(k+2) = A(\omega)\hat{i}(k+1) + BV(k+1) \tag{4}$$

where $A = C + G$ is introduced for clarity. The predicted control error is then given by

$$\hat{e}(k+2) = I_s^*(k+2) - \left(A(\omega)\hat{i}(k+1) + BV(k+1)\right) \tag{5}$$

2.5. Cost Function

In a general MPC application, the CF incorporates various terms. The primary one constitutes a penalization of output variables from their references. Additional terms include penalization of control effort and other objectives. In FSMPC stator current control, typically, predicted control errors and VSI switching events are penalized in the following manner [22]:

$$J(k+2) = \hat{e}_{\alpha-\beta}^2(k+2) + \lambda_{xy}\hat{e}_{x-y}^2(k+2) + \lambda_{sc}\Delta S(k+1) \tag{6}$$

where $\Delta S(k+1)$ represents the number of switch transitions at the VSI when the configuration $u(k)$ is changed to $u(k+1)$. For single-vector approaches, the value of $\Delta S(k+1)$ can be calculated as

$$\Delta S(k+1) = \sum_{i=1}^{5} |u_i(k+1) - u_i(k)| \tag{7}$$

With this cost function structure, the weighting factors (WFs) are the parameters λ_{xy} and λ_{sc}. The first parameter emphasizes the reduction of x-y currents, while the second helps minimize the switching frequency.

2.6. Optimization and Deployment

In FSMPC, the control move for the $k+1$ period is determined at discrete time k as $u^{opt} = \text{argmin} J(k+2)$. In earlier studies, the optimization phase of FCSMPC was performed by exhaustive search. This involved computing the value of J for each candidate or allowed control move to obtain the minimum.

The deployment of the method in a DSP is relatively straightforward. A flowchart of the FSMPC algorithm is shown in Figure 3. It is interesting to note that the main blocks are the same regardless of the type of machine (induction, permanent magnet, etc.) and regardless of the number of phases. For any particular case, one needs just to adjust the model and a few parameters.

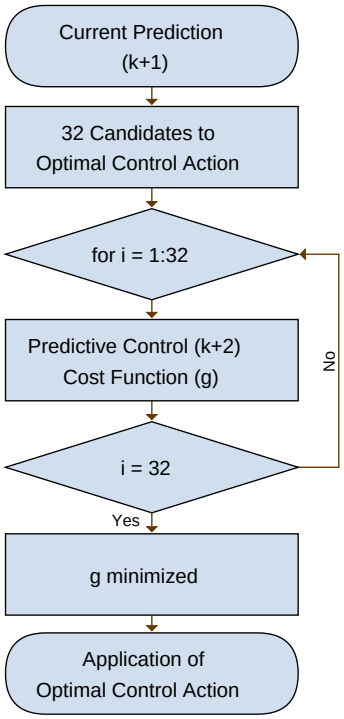


Figure 3. Flowchart for FSMPC of stator current.

The results of FSMPC have been featured in many papers [4]. In the case of MPS, special attention must be given to the different planes in the VSD decomposition. As an example, check the waveforms in Figure 4, where the α-β components clearly follow their sinusoidal references and the x-y components are regulated around zero.

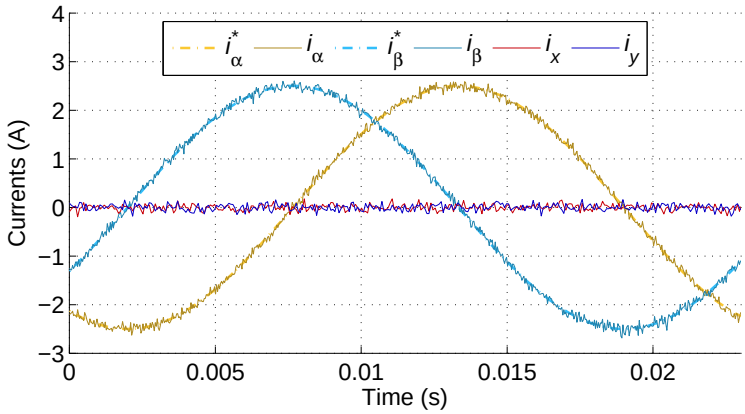


Figure 4. Typical evolution of stator currents for FSMPC.

Despite the flexibility of FSMPC, its practical application is hindered by a significant computational load, especially in MPS, due to the large number of possible control moves. As discussed in the Introduction, a high computational load leads to a reduced sampling frequency, which in turn limits the control bandwidth. Additionally, in the case of single-vector approaches, the longer duration of the applied voltages results in significant distortion from the ideal sinusoidal waveform.

This issue prompted researchers to explore methods for reducing the time required for the optimization phase. The various approaches developed are categorized in the next section.

3. Fast Computation Strategies

Numerous FSMPC proposals for MPS address the issue of fast computation. Some of these approaches combine multiple strategies. For example, in the context of Virtual Voltage Vectors, techniques such as control set reduction, elimination of weighting factors, and cost function simplification can be found. To provide a meaningful classification, the following fundamental techniques are considered.

3.1. Reduction of the Allowed Control Set

The candidate control moves considered during the optimization phase form the Allowed Control Set (ACS). In single-vector FSMPC, this set is typically a subset of the complete set of VSI configurations. In multi-vector FSMPC, the ACS represents a subset of all possible sequences. To maintain clarity, the single-vector case will be discussed first. In this approach, the ACS is often composed of two or more basic VV subsets (e.g., LVV, MVV, etc.). A specific example involves the combination of the LVV set and the ZVV set, introduced in [10].

Using this idea, ref. [23] introduces an advanced FCS-MPC. This method employs Virtual Voltage Vectors that automatically suppress third harmonic currents, simplifying the cost function by omitting harmonic terms. Furthermore, an Adaptive Control Set dynamically adjusts Voltage Vector amplitudes based on rotor speed, significantly enhancing performance at low speeds. To ensure stability, delay compensation predicts the system state for the next control interval. By achieving an optimal balance between precision and computational efficiency, this approach is highly suitable for demanding applications such as electric vehicle propulsion.

Likewise, an optimized MPC strategy is proposed in [24], focusing on overcoming the operational performance and computational challenges of traditional methods. The approach introduces a set of 24 Virtual Voltage Vectors uniformly distributed to improve control precision by offering a denser selection of candidates. A novel minimum error duty cycle calculation is included to optimize the relationship between the selected Voltage Vectors and reference currents in the d-q axes, minimizing tracking errors. To reduce computational effort, a multi-stage evaluation method is developed, simplifying the vector selection process and reducing the number of evaluations from 24 to 8 cycles.

A preselection based on deviation in stator current and the change in stator current vector is proposed in [25]. The direction and magnitude of per-unit current vector is considered for a region identification procedure, resulting in a large reduction in computing needs. However, just d_3-q_3 harmonic currents are considered.

3.2. Simplification of the CF and Search Method

Another strategy to accelerate the computation of the control signal in FSMPC for MPS focuses on simplifying the optimization problem, achieved through two primary approaches. The first approach simplifies the cost function by reducing the number of terms, including methods that eliminate the need for a weighting factor (WF). The second streamlines the search process by limiting the exploration of the full set of possible control actions, effectively pruning the search tree. It is crucial to highlight that these strategies do not reduce the number of ACSs; instead, they optimize the selection process for efficiency.

A method for six-phase PMSM is presented in [26], employing two groups of Virtual Vectors with varying magnitudes. This approach improves torque regulation and eliminates the need for weighting factor tuning in the cost function. Additionally, a one-step lookup table is introduced to exclude unnecessary Voltage Vectors, significantly reducing computation time.

Other authors propose a Model-Free Predictive Control (MF-PC) algorithm that eliminates complex operations such as multiplications and parameter estimation, providing enhanced accuracy and robustness to parameter variations while maintaining low computational complexity. Ref. [27] demonstrates that the method can effectively manage load disturbances and parameter mismatches, achieving reduced harmonic distortion and

torque ripple. It highlights the advantages of a parameter-independent control strategy that avoids the computational burden of traditional approaches while maintaining high precision. Ref. [28] introduces the ABC frame for multi-phase systems, which predicts control actions independently for each phase. By avoiding the need for frame transformations and weighting factors, this approach significantly reduces computational burdens. Simulations and experiments demonstrate its effectiveness, achieving comparable performance to traditional methods while improving efficiency, particularly in systems with multiple phases.

Regarding WF elimination, it naturally occurs in Virtual Voltage Vector (VVV) approaches, as x-y currents do not need to be included in the cost function, and switching becomes more predictable. Other works explicitly perform WF elimination, such as in [29–31]. Additionally, some approaches focus on the design of parameter-free cost functions, as seen in [32,33].

Restrained Search Predictive Control (RSPC) is a technique presented in [34] that reduces computational complexity by limiting the number of inverter switching states that can be evaluated in each sampling cycle. Instead of exhaustively analyzing all possible switching combinations, RSPC imposes constraints that select only a subset of switching vectors, thereby reducing the number of phase changes in the inverter. This approach lowers switching losses and improves system efficiency.

RSPC focuses on two main restrictions: selecting only those vectors that involve one or no commutations per cycle and preventing any inverter phase from switching in two consecutive cycles. These constraints facilitate real-time implementation, enhance drive efficiency, and reduce the maximum switching frequency, which is especially advantageous in high-power applications and complex multi-phase systems.

Improved techniques of RSPC is presented in [35] for multi-phase drives, where the commutations of VSI are minimized, favoring the drive efficiency.

On the other hand, ref. [36] presents a computationally efficient multi-step direct predictive torque control (M-DPTC) for surface-mounted permanent magnet synchronous motors (SPMSMs). The method uses a simplified predictive model and a novel optimization approach to reduce computational complexity, achieving logarithmic time growth instead of exponential. By utilizing lookup tables and addition operations, the algorithm avoids exhaustive computations, enabling real-time implementation within short sample periods. Experimental and simulation results validate its effectiveness in reducing switching frequency and losses while maintaining steady and dynamic performance.

A novel technique, introduced in [37], proposes a dual second-order MPC strategy. This approach enhances flexibility in controlling Voltage Vector direction and amplitude, reduces torque and current ripples, and improves steady-state performance. By applying second-order MPC to both speed and current loops, the system achieves faster response times and reduced overshoot compared to traditional PI control. The method employs four-vector space vector PWM (SVPWM) modulation, optimizing the current loop while maintaining minimal computation requirements, as validated through simulations and experiments.

The approach presented in [38] explores two modified MPC strategies designed to enhance the control of asymmetric six-phase PMSMs. The first method integrates MPC within the conventional cascaded speed–current control loop, replacing the current control with MPC to achieve faster response times and reduce harmonic currents. The second method eliminates the cascaded loops entirely, consolidating both speed and current control into a single MPC, which improves the system's dynamic performance and flexibility. Both approaches utilize Vector Space Decomposition (VSD) to isolate torque-producing components and suppress non-torque harmonics, thereby optimizing the Maximum Torque per Ampere (MTPA) operation and enhancing efficiency in multi-phase systems.

An improved control scheme for five-phase PMSMs that enhances tracking accuracy and DC-link voltage utilization while reducing computational load is presented in [39]. It employs a double-vector method where two optimal voltage vectors are selected online

during each sampling interval, paired with duty ratio optimization to improve tracking precision in two subspaces (α-β and x-y). By limiting the candidate vectors to only the five nearest ones in the reference sector, the method drastically reduces the computational requirements compared to traditional schemes, enabling practical real-time implementation without sacrificing performance.

Another approach presents a hybrid exploration state method [40] that combines four-state and seven-state exploration techniques by dividing the space vector plane into regions based on the reference Voltage Vector's magnitude and angle. Key benefits include reduced RMS current ripple compared to conventional methods; optimized computational effort, minimizing processing load versus the seven-state method; and improved switching frequency balance, ensuring efficient and stable motor control. This method offers a practical and efficient solution for applications demanding high-precision motor control.

3.3. Explicit MPC

Reducing the computational load has been tackled by resorting to general optimization methods, some of which have proven effective in cases where control actions are quantized, as in FSMPC. In Explicit Model Predictive Control (EMPC) [41], a quadratic optimization problem is decomposed into multiple local subproblems, with their solutions computed offline. Implementing EMPC involves identifying the relevant subproblem (via region determination) and retrieving the appropriate control law from a precalculated table [42,43]. One of the main challenges with reported EMPC applications is the application of a general region-splitting methodology that lacks physical insight, leading to unnecessarily high complexity. Additionally, the inclusion of complex cost functions can make the EMPC problem more challenging.

Another general technique is the Sphere Decoding Optimization algorithm [44]. Likewise, Laguerre function-based MPC with a modulator has been proposed for long-horizon problems [45]. However, these methods focus on long horizons and do not completely eliminate the need for combinatorial search.

3.4. Dead-Beat Approach

Dead-beat control is enabled by direct digital control of dynamical systems. The basic idea is to apply a control action that, after one sampling period, will drive the error to zero. Its application to drives can be traced back to the 1980s [46]. In the case of FSMPC, using Equation (5), one can derive the voltage that, applied during the $k+1$ interval, would drive the error to zero at $k+2$. Denoting it by V^*, it turns out to be

$$V^* = B^{-1}\big(i^*(k+2) - A(\omega)\hat{i}(k+1)\big). \tag{8}$$

Voltage V^* might not be one of the 32 VVs that the VSI can produce. Then it must be synthesized using various basic VVs applied at different times and for different subperiods during the whole sampling period. The basic VVs that need be applied can be found using trigonometric rules and lookup tables [47,48]. Different approaches have appeared using the DB concept. They have been applied to different types of drives and numbers of phases.

3.5. Region-Based Methods

FSMPC based on regions can be seen as a particular case of EMPC where the regions are determined using physical insight. The idea can be put forward for the single-vector case using the following observation. Minimizing J amounts to minimizing $\|V^* - V^h\|_w^2$, where index h goes from 1 to the number of available VVs. This can be checked noting that $\hat{e} = i^* - \hat{i}$ with $\hat{i} = A(\omega)\hat{i}(k+1) + BV^h$ for some basic VVs of index h. As a result, the following identity is found:

$$B^{-1}\hat{e} = B^{-1}\big(i^* - A(\omega)\hat{i}(k+1)\big) - V^h, \tag{9}$$

where the right-hand side is exactly $V^* - V^h$ by definition. So, the term $\hat{e}$ can be replaced by $B(V^* - V^h)$ in the expression of the cost function. Now, B does not depend on the VV selected, so minimizing J and minimizing $\|V^* - V^h\|_w^2$ yields the same result.

From this, one can resort to Voronoi regions to provide a convenient way for $\|V^* - V^h\|_w$ minimization. In fact, the cumbersome exhaustive exploration is avoided. Voronoi regions appear because $\|V^* - V^h\|_w$ defines a metric in the mathematical sense [49]. Then, to compute the VV minimizing the cost function, one just needs to find in which Voronoi region V^* is placed. The application of these ideas to MPS first appeared in [50] for a reduced cost function.

4. Critical Analysis and Discussion

In this section, the previously introduced strategies are compared by analyzing selected papers. A classification is used to proceed in an orderly manner. The taxonomy uses as the main characteristic the number of VVs issued per sampling period. The multi-vector class is first reviewed, as it has contributed earlier to the development of fast optimization methods. Figure 5 shows a schematic diagram for the reviewed strategies. The reviewed papers are classified accordingly, as shown in Table 1.

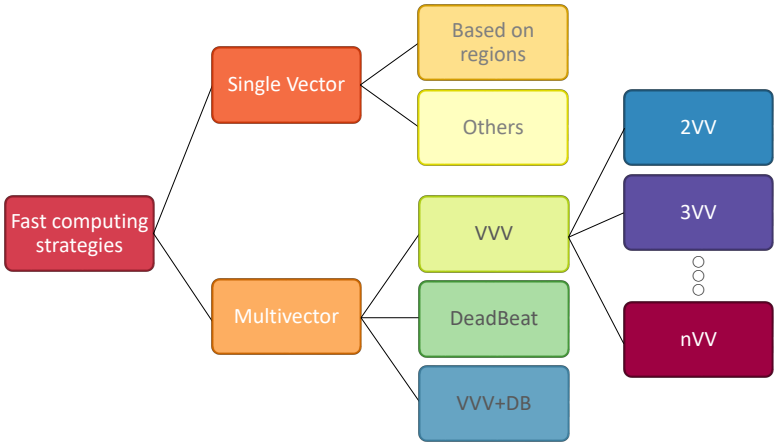


Figure 5. Categorization of fast computing strategies for FSMPC.

Table 1. Taxonomy of FSMPC for MPS regarding computational reduction.

Single vector	Regions	[40–44,50–61]
	Others	[10,24,25,28–37]
Multi-vector	2 VVVs	[26,39,55,62–67]
	3 VVVs	[68–70]
	4 VVVs or more	[19,23–25,34,38,47,71–78]
	Dead-beat	[46–48,69,79–83]
	VVV+DB	[70,84–86]

4.1. Multi-Vector Approaches

Multi-vector methods in FSMPC are characterized by the application of more than one basic VV per sampling period. Early studies combined a non-zero VV with a Null VV to produce an average voltage with a reduced magnitude compared to that of the basic non-zero VV. In this way, the modulus of the voltage is affected so that a closer approximation to V^* is found [62]. Subsequently, this concept was expanded to include combinations of two non-zero VVs, generating an average voltage with specific benefits for certain applications.

In MPS, certain combinations of basic VVs can yield a zero average voltage in the x-y plane, minimizing x-y excitation. This allows the x-y terms to be omitted from the cost function, simplifying the computation. Additionally, the set of Virtual VVs is smaller than the complete VV set, reducing the enumeration process needed to optimize the cost function. Further constraints on the VVV sequence can reduce the optimization search space even more [51].

The VVV approach has been applied to various types of multi-phase systems [63,68]. For example, ref. [47] explores using adjacent VVVs and the vector opposite to the previous optimal one, reducing the exhaustive search to only five evaluations. This method is demonstrated on a two-level, five-phase PMSM system.

In terms of experimental application, a limitation of VVV methods is that they manage x-y currents in open-loop. Factors such as switch dead time, machine asymmetries, and back-EMF harmonics can lead to unwanted x-y currents, increasing copper losses. Another issue concerns DC bus utilization, as combinations of basic VVs do not provide the same voltage range as individual basic VVs [87]. To address these concerns, [88] proposed a method using dual VVVs for α-β control while regulating x'-y' currents without interference.

Closely related to VVVs are multi-vector methods incorporating the dead-beat concept. These aim at generating an average voltage exactly matching V^* by combining basic VVs during a single sampling period. The work of [40] uses DB with hybrid-state exploration to reduce computational load and current ripple. In [89], a similar approach is used with asymmetric space vector PWM. The method in [71] applies two VVs per period, switching in just two phases and evaluating only six candidate VVs at each period. Ref. [90] extends the DB concept to a multi-variable approach controlling all variables within a single predictive loop. Further variations are explored in [48,69,91–95].

Despite its advantages, the DB approach has limitations in terms of experimental application. First, the goal of exact cancellation of the control error is practically unachievable due to unmodeled dynamics and parameter variations. Furthermore, the synthesis of V^* from multiple VVs leads to the average deception problem because the optimal voltage acts only as an average over the sampling period [87]. This issue affects the trade-offs between α-β tracking and x-y regulation, which are particularly significant in multi-phase systems, as x-y currents lead to additional losses [72,96,97].

Another concern for experimental application of DB schemes is the switching frequency. DB methods often require more frequent changes in the VSI configuration than single-vector approaches. For example, ref. [73] limits switching by selecting four VVs per sampling period from a lookup table that restricts the number of commutations, thereby reducing the Average Switching Frequency (AFS).

Another aspect, related to the actual implementation, is that DB-FSMPC methods often rely on trigonometric functions to determine the VV combination. These functions can be computationally intensive and unreliable at times, and they may not be feasible on low-end hardware.

4.2. Single Vector

From a practical application point of view, single-vector predictive methods face computational challenges. This is especially notable in MPS, as the number of basic VVs grows exponentially with the number of phases [47]. The usual approach to SV-FSMPC is the exhaustive search optimization of the cost function. The computational load is then high, leading to high sampling periods. This reduces the bandwidth of the stator current control.

Early methods for computational load reduction relied on procedures that reduced the capabilities of SV-FSMPC. For instance, reducing the allowed VVs makes modulation more challenging in some regions of the operating space [10]. Elimination of WFs reduces the flexibility to cope with conflicting objectives. Finally, restrained search produces solutions that are not guaranteed to be optimal.

A recent development in SV-FSMPC for MPS is the introduction of a region-based method [50]. This approach extends prior works developed for VVVs, such as [52–56].

However, ref. [50] only considers the α-β plane, which leads to the generation of x-y currents. This problem is eliminated in [57], where a region-based method is proposed. The method enables the use of a weighting factor for x-y content management.

A similar approach is found late in [58], where current error magnitude and sign alongside the current gradient are used to assess error tendencies.

In these methods, the VV application time is equal to the entire sampling period. This results in increased harmonic distortion in stator currents. Non-uniform sampling has been proposed in FSMPC by dividing the sampling period into subintervals, allowing both VV selection and application time optimization within a single sampling period [59]. However, the computational load increases considerably. In [60], a region-based method is proposed using variable application times. Both the VV and its application time are found without exhaustive search.

These recent advances make FSMPC competitive and, arguably, superior to multi-vector solutions, especially considering the ability of SV-FSMPC to incorporate weighting factors in the CF.

4.3. Trade-Offs in Weighting Factors Tuning

Weighting factors allow putting more emphasis on different objectives. One criticism often placed on WF use is that their tuning is difficult [98]. This has prompted both the development of WF-free methods [99] and proposals for WF selection [100].

The first systematic approach to WF tuning in MPS was proposed by [96], introducing a Pareto-front approach for a six-phase IM. This approach was later expanded in [101] using a multi-objective genetic algorithm for predictive torque control of a six-phase IM, though it overlooked x-y plane issues. Other techniques, like NSGA-II with TOPSIS, are applied to WF tuning for conventional IM in [102], though they are limited to load conditions. A multi-objective particle swarm optimization is used in [97] to address both x-y currents and switching frequency. Some methods also incorporate artificial intelligence, such as the neural network approach in [103] for two WFs in permanent magnet drives, relying on simulation and limited experimental cases.

Distinct from these, ref. [22] introduces an adaptive cost function for VSD using a six-phase IM, where performance metrics are explicitly linked to WFs. This adaptive approach characterizes the Pareto front with a single equation, enabling straightforward rule-based adaptation without the computational overhead of genetic or swarm algorithms.

Recent online WF tuning methods for various VSDs are based on the idea of gain-scheduling, treating the WFs as the gains [104]. More complex algorithms have also been proposed. For instance, ref. [105] applies reinforcement learning to tune WFs in PTC for permanent magnet motors. Although innovative, reinforcement learning requires extensive data.

In [106], the first variable WF method for drives demonstrates the non-linear relationship between performance indicators and speed. The proposal has some limitations: it does not calculate the actual WFs, it uses TOPSIS at every sampling period rather than adapting only when conditions change, it lacks a clear connection between WFs and performance metrics, an it requires tuning of hyperparameters, preventing full automation. Note that the trade-offs considered in most studies concern just electrical variables [107]. Alternatively, ref. [108] optimizes a single WF for each sampling period in PTC of a three-phase IM yet fails to link performance metrics directly to WFs.

Advances in hardware have significantly influenced this field, particularly with the introduction of new power converter technologies such as silicon carbide (SiC) and gallium nitride (GaN). These converters enable higher switching frequencies, reducing the emphasis on switching penalty terms in cost functions. However, methods employing weighting factors (WFs) can trade off switching frequency to optimize performance [109,110], whereas in other approaches, the switching frequency remains relatively fixed [74]. In addition to the above, the field still has to face the challenges of concurrent tuning of both loops in the IFOC scheme [111].

A final remark can be made regarding computation times for each algorithm. The reported values are different from one publication to another. This is to be expected since many factors affect these figures. The capabilities of the hardware, the expertise in coding, and the number of phases are the main ones. Nevertheless there is a clear distinction between recent fast methods and previous ones. Both in the single-vector and multi-vector cases, the computational load reduction of region-based methods is larger that that of previous methods. This is highlighted in Table 2, where the reported computation times are presented.

Table 2. Reported computation times for some FSMPC techniques.

Strategies		Load (µs)	Reference
Single vector	Regions	9	[50]
	Others	24.16	[29]
Multi-vector	2 VVVs	45.8	[26]
	3 VVVs	65	[70]
	4 VVVs	27.6	[47]
	Dead-beat	50.36	[83]
	VVV+DB	40.23	[84]

5. Conclusions

The development of fast computational strategies has transformed FSMPC for multi-phase drives, achieving significant reductions in sampling periods without requiring advanced hardware. Key innovations, such as reducing the ACS and simplifying cost functions, have streamlined complex computations while maintaining high control performance. Techniques like VVVs and lookup tables preselect optimal voltage candidates, minimizing the need for exhaustive searches.

This paper shows that the main battlefields are those of multi-vector and single-vector, each offering unique strengths and trade-offs. Multi-vector strategies enhance precision by combining vectors to improve control accuracy, making them suitable for high-performance systems. Conversely, single-vector methods prioritize simplicity and computational efficiency, making them ideal for applications with limited resources or real-time constraints.

Furthermore, paradigms such as region-based methods and DB control have further enhanced FSMPC's efficiency. Region-based techniques use Voronoi diagrams to bypass exhaustive searches, while DB control predicts system states to minimize errors within a single sampling period. These methods, alongside hybrid strategies, ensure FSMPC's adaptability to increasingly complex and demanding applications, such as electric vehicles and renewable energy.

These advancements promise not only to refine predictive control methodologies but also to extend their application to more complex and demanding multi-phase drive systems. This evolution underscores the ongoing innovation and dynamic problem-solving required to meet the challenges of modern power electronics.

Author Contributions: M.R.A. provided conceptualization and wrote the first draft; E.M. reviewed, wrote the first draft, and improved the structure of the paper; M.G.S. and M.P. contributed to reviewing and editing the paper. All authors have read and agreed to the published version of the manuscript.

Funding: This research is part of Proyecto I+D+i/PID2021-125189OB-I00 funded by MICIU/AEI/10.13039/501100011033 and FEDER, UE.

Institutional Review Board Statement: Not applicable.

Informed Consent Statement: Not applicable.

Data Availability Statement: Not applicable.

Conflicts of Interest: The authors declare no conflicts of interest. The funders had no role in the design of the study; in the collection, analyses, or interpretation of data; in the writing of the manuscript; or in the decision to publish the results.

Abbreviations

The following abbreviations are used in this manuscript:

ACS	Allowed Control Set
AC	Alternating current
AFS	Average Switching Frequency
CF	Cost function
DB	Dead-beat
DC	Direct current
FCS	Finite Control Set
FSMPC	Finite-State Model Predictive Control
IFOC	Indirect Field-Oriented Control
IM	Induction motor
LVV	Large Voltage Vector
MTPA	Maximum Torque per Ampere
MVV	Medium Voltage Vector
MF-PC	Model-Free Predictive Control
MPC	Model Predictive Control
MPS	Multi-Phase Systems
NVV	Null Voltage Vector
PMSM	Permanent Magnet Synchronous Motor
PID	Proportional Integral Derivative
RSPC	Restrained Search Predictive Control
SVV	Small Voltage Vector
TOPSIS	Technique for Order of Preference by Similarity to Ideal Solution
VSD	Vector Space Decomposition
VVV	Virtual Voltage Vector
VSI	Voltage Source Inverter
VV	Voltage Vector
WF	Weighting factor

References

1. Rault, J.; Richalet, A.; Testud, J.; Papon, J. Model predictive heuristic control: Application to industrial processes. *Automatica* **1978**, *14*, 413–428.
2. Limon, D.; Ferramosca, A.; Alvarado, I.; Alamo, T. Nonlinear MPC for tracking piece-wise constant reference signals. *IEEE Trans. Autom. Control* **2018**, *63*, 3735–3750. [CrossRef]
3. Holtz, J.; Stadtfeld, S. *A Predictive Controller for the Stator Current Vector of AC Machines Fed from a Switched Voltage Source*; JIEE IPEC-Tokyo: Tokyo, Japan, 1983; pp. 1665–1675.
4. Lim, C.S.; Levi, E.; Jones, M.; Rahim, N.A.; Hew, W.P. A comparative study of synchronous current control schemes based on FCS-MPC and PI-PWM for a two-motor three-phase drive. *IEEE Trans. Ind. Electron.* **2014**, *61*, 3867–3878. [CrossRef]
5. Arahal, M.R.; Barrero, F.; Ortega, M.G.; Martin, C. Harmonic analysis of direct digital control of voltage inverters. *Math. Comput. Simul.* **2016**, *130*, 155–166. [CrossRef]
6. Tenconi, A.; Rubino, S.; Bojoi, R. Model predictive control for multiphase motor drives—A technology status review. In Proceedings of the 2018 International Power Electronics Conference (IPEC-Niigata 2018-ECCE Asia), Niigata, Japan, 20–24 May 2018; pp. 732–739.
7. Levi, E. Multiphase electric machines for variable-speed applications. *IEEE Trans. Ind. Electron.* **2008**, *55*, 1893–1909. [CrossRef]
8. Elmorshedy, M.F.; Xu, W.; El-Sousy, F.F.; Islam, M.R.; Ahmed, A.A. Recent Achievements in Model Predictive Control Techniques for Industrial Motor: A Comprehensive State-of-the-Art. *IEEE Access* **2021**, *9*, 58170–58191. [CrossRef]
9. Zhao, Y.; Lipo, T.A. Space vector PWM control of dual three-phase induction machine using vector space decomposition. *IEEE Trans. Ind. Appl.* **1995**, *31*, 1100–1109. [CrossRef]
10. Arahal, M.R.; Barrero, F.; Toral, S.; Durán, M.J.; Gregor, R. Multi-phase current control using finite-state model-predictive control. *Control Eng. Pract.* **2009**, *17*, 579–587. [CrossRef]

11. Li, Z.; Guo, Y.; Xia, J.; Li, H.; Zhang, X. Variable sampling frequency model predictive torque control for VSI-fed IM drives without current sensors. *IEEE J. Emerg. Sel. Top. Power Electron.* **2020**, *9*, 1507–1517. [CrossRef]
12. Fan, Y.; Tong, L.; Lu, Y.; Cai, X.; Fu, Z.; Mao, X. High-Switching-Frequency SiC Power Conversion Systems with Improved Finite Control Set Method Prediction Control. *Energies* **2024**, *17*, 4601. [CrossRef]
13. Abdel-Moneim, M.G.; Abdel-Azim, W.E.; Abdel-Khalik, A.S.; Hamed, M.S.; Ahmed, S. Model Predictive Current Control of Nine-Switch Inverter-Fed Six-Phase Induction Motor Drives Under Healthy and Fault Scenarios. *IEEE Trans. Transp. Electrif.* **2024**. [CrossRef]
14. Schirone, L.; Macellari, M.; Pellitteri, F. Predictive dead time controller for GaN-based boost converters. *IET Power Electron.* **2017**, *10*, 421–428. [CrossRef]
15. Tang, S.; Wang, J.; Wang, D.; Zhang, C.; Yin, X.; Shuai, Z.; Shen, Z.J. Vector analysis based multiobjective-modulated model predictive control for four-switching-state multilevel converters. *IEEE Trans. Ind. Electron.* **2021**, *69*, 12999–13010. [CrossRef]
16. Kulandaivel, G.; Sundaram, E.; Gunasekaran, M.; Chenniappan, S. Five-phase induction motor drive-a comprehensive review. *Front. Energy Res.* **2023**, *11*, 1178169. [CrossRef]
17. Barrero, F.; Satué, M.G.; Colodro, F.; Arahal, M.R. Tuning of Modern Speed Drives Using IFOC: A Case Study for a Five-Phase Induction Machine. *Results Eng.* **2024**, *24*, 103145. [CrossRef]
18. Nie, Z.; Schofield, N. Multi-phase VSI DC-link capacitor considerations. *IET Electr. Power Appl.* **2019**, *13*, 1804–1811. [CrossRef]
19. Xue, C.; Song, W.; Feng, X. Finite control-set model predictive current control of five-phase permanent-magnet synchronous machine based on virtual voltage vectors. *IET Electr. Power Appl.* **2017**, *11*, 836–846. [CrossRef]
20. Rodas, J.; Barrero, F.; Arahal, M.R.; Martín, C.; Gregor, R. Online estimation of rotor variables in predictive current controllers: A case study using five-phase induction machines. *IEEE Trans. Ind. Electron.* **2016**, *63*, 5348–5356. [CrossRef]
21. Satué, M.G.; Arahal, M.R.; Ramírez, D.R. Rotor Current Estimation in Predictive Control of Multi-phaseDrives. *Rev. Iberoam. AutomÁtica InformÁtica Ind.* **2023**, *20*, 25–31.
22. Arahal, M.R.; Satué, M.G.; Barrero, F.; Ortega, M.G. Adaptive Cost Function FCSMPC for 6-Phase IMs. *Energies* **2021**, *14*, 5222. [CrossRef]
23. Wang, W.; Fan, Y.; Chen, S.; Zhang, Q. Finite control set model predictive current control of a five-phase PMSM with virtual voltage vectors and adaptive control set. *CES Trans. Electr. Mach. Syst.* **2018**, *2*, 136–141. [CrossRef]
24. Cui, J.; Tao, T.; Zhao, W. Optimized Control Set Model Predictive Control for Dual Three Phase PMSM With Minimum Error Duty Cycle Regulation. *IEEE Trans. Power Electron.* **2023**, *39*, 1319–1332. [CrossRef]
25. Rajanikanth, P.; Parvathy, M.; Thippiripati, V.K. Enhanced Model Predictive Current Control based Five-Phase PMSM Drive. *IEEE J. Emerg. Sel. Top. Power Electron.* **2023**, *12*, 838–848. [CrossRef]
26. Luo, Y.; Liu, C. A Flux Constrained Predictive Control for a Six-Phase PMSM Motor with Lower Complexity. *IEEE Trans. Ind. Electron.* **2019**, *66*, 5081–5093. [CrossRef]
27. Huang, W.; Huang, Y.; Xu, D. Model-Free Predictive Current Control of Five-Phase PMSM Drives. *Electronics* **2023**, *12*, 4848. [CrossRef]
28. Mousavi, M.S.; Davari, S.A.; Flores, F.; Garcia, C.; Rodriguez, J. ABC Frame Model-Free Predictive Control for Multiphase Converters and Electrical Drives. In Proceedings of the 2023 IEEE International Conference on Predictive Control of Electrical Drives and Power Electronics (PRECEDE), Wuhan, China, 16–19 June 2023; pp. 1–6.
29. Serra, J.; Cardoso, A.J.M. A Simplified Model Predictive Control for Asymmetrical Six-Phase Induction Motors That Eliminates the Weighting Factor. *Machines* **2022**, *10*, 1189. [CrossRef]
30. Mirzaeipour, P.; Saniei, M. Software Evaluation of Reducing the Number of Switching States and Removing the Weight Factor in the Predictive Current Control of Six-Phase Induction Motor. *Nashriyyah-I Muhandisi-I Barq Muhandisi-I Kampyutar-I Iran* **2023**, *99*, 245.
31. Rodas, J.; González, O.; Norambuena, M.; Doval-Gandoy, J.; Gomis-Bellmunt, O.; Gregor, R.; Ayala, M.; Rodríguez, J.; Romero, C. Weighting-Factorless Sequential Model Predictive Torque Control of a Six-Phase AC Machine. In Proceedings of the 2023 IEEE Conference on Power Electronics and Renewable Energy (CPERE), Luxor, Egypt, 19–21 February 2023; pp. 1–5.
32. Eshwar, K.; Thippiripati, V.K. Weighting-factorless predictive torque control scheme for dual inverter fed open-end-winding PMSM with single DC source. *IEEE Trans. Power Electron.* **2021**, *36*, 12968–12978. [CrossRef]
33. Jayan, V.; Ghias, A.M. Weighting Factor Free Model Predictive Control for a Flying Capacitor Converter in a DC Microgrid. *IEEE Trans. Energy Convers.* **2021**, *37*, 1030–1041. [CrossRef]
34. Durán, M.; Prieto, J.; Barrero, F.; Toral, S. Predictive Current Control of Dual Three-Phase Drives Using Restrained Search Techniques. *Ind. Electron. IEEE Trans.* **2011**, *58*, 3253–3263. [CrossRef]
35. Durán, M.; Barrero, F.; Toral, S.; Arahal, M.; Prieto, J. Improved techniques of restrained search predictive control for multiphase drives. In Proceedings of the 2009 IEEE International Electric Machines and Drives Conference, Miami, FL, USA, 3–6 May 2009; pp. 239–244.
36. Xia, C.; Zhou, Z.; Wang, Z.; Yan, Y.; Shi, T. Computationally efficient multi-step direct predictive torque control for surface-mounted permanent magnet synchronous motor. *IET Electr. Power Appl.* **2017**, *11*, 805–814. [CrossRef]
37. Li, L.; Zhou, W.; Bi, X.; Sun, X.; Shi, X. Second-Order Model-Based Predictive Control of Dual Three-Phase PMSM Based on Current Loop Operation Optimization. *Actuators* **2022**, *11*, 251. [CrossRef]

38. Ye, D.; Li, J.; Qu, R.; Lu, H.; Lu, Y. Finite set model predictive MTPA control with VSD method for asymmetric six-phase PMSM. In Proceedings of the 2017 IEEE International Electric Machines and Drives Conference (IEMDC), Miami, FL, USA, 21–24 May 2017; pp. 1–7. [CrossRef]
39. Saeed, M.S.R.; Song, W.; Huang, L.; Yu, B. Double-Vector-Based Finite Control Set Model Predictive Control for Five-Phase PMSMs with High Tracking Accuracy and DC-Link Voltage Utilization. *IEEE Trans. Power Electron.* **2022**, *37*, 15234–15244. [CrossRef]
40. Abbaszadeh, A.; Arab Khaburi, D.; Kennel, R.; Rodríguez, J. Hybrid exploration state for the simplified finite control set-model predictive control with a deadbeat solution for reducing the current ripple in permanent magnet synchronous motor. *IET Electr. Power Appl.* **2017**, *11*, 823–835. [CrossRef]
41. Alessio, A.; Bemporad, A. A survey on explicit model predictive control. In *Nonlinear Model Predictive Control*; Springer: Berlin/Heidelberg, Germany, 2009; pp. 345–369.
42. Zhao, M.; Cao, Y.; Yan, Y.; Zhang, Z.; Shi, T.; Xia, C. Weighting Factors Tuning Method in Explicit Model Predictive Direct Speed Control of Permanent Magnet Synchronous Motor. In Proceedings of the 2021 24th International Conference on Electrical Machines and Systems (ICEMS), Gyeongju, Republic of Korea, 31 October–3 November 2021; pp. 653–658.
43. Belda, K.; Píša, P. Explicit Model Predictive Control of PMSM Drives. In Proceedings of the 2021 IEEE 30th International Symposium on Industrial Electronics (ISIE), Kyoto, Japan, 20–23 June 2021; pp. 01–06.
44. Grimm, F.; Kolahian, P.; Zhang, Z.; Baghdadi, M. A sphere decoding algorithm for multistep sequential model-predictive control. *IEEE Trans. Ind. Appl.* **2021**, *57*, 2931–2940. [CrossRef]
45. Xu, Y.; Li, S.; Zhang, W.; Yu, G.; Zou, J. Long-horizon constrained model predictive direct speed control for PMSM drives based on laguerre functions. *IEEE Trans. Control. Syst. Technol.* **2023**, *32*, 1002–1014. [CrossRef]
46. Kawabata, T.; Miyashita, T.; Yamamoto, Y. Dead beat control of three phase PWM inverter. In Proceedings of the 1987 IEEE Power Electronics Specialists Conference, Blacksburg, VA, USA, 21–26 June 1987; pp. 473–481.
47. Yu, B.; Song, W.; Yang, K.; Guo, Y.; Saeed, M.S.R. A Computationally Efficient Finite Control Set Model Predictive Control for Multiphase PMSM Drives. *IEEE Trans. Ind. Electron.* **2022**, *69*, 12066–12076. [CrossRef]
48. Serra, J.; Jlassi, I.; Cardoso, A.J.M. A computationally efficient model predictive control of six-phase induction machines based on deadbeat control. *Machines* **2021**, *9*, 306. [CrossRef]
49. Aurenhammer, F.; Klein, R. Voronoi Diagrams. *Handb. Comput. Geom.* **2000**, *5*, 201–290.
50. Arahal, M.R.; Barrero, F.; Satué, M.G.; Bermúdez, M. Fast finite-state predictive current control of electric drives. *IEEE Access* **2023**, *11*, 12821–12828. [CrossRef]
51. Ayala, M.; Doval-Gandoy, J.; Rodas, J.; Gonzalez, O.; Gregor, R. Current control designed with model based predictive control for six-phase motor drives. *ISA Trans.* **2020**, *98*, 496–504. [CrossRef] [PubMed]
52. Nemec, M.; Drobnic, K.; Nedeljkovic, D.; Ambrozic, V. Direct current control of a synchronous machine in field coordinates. *IEEE Trans. Ind. Electron.* **2009**, *56*, 4052–4061. [CrossRef]
53. Xia, C.; Liu, T.; Shi, T.; Song, Z. A simplified finite-control-set model-predictive control for power converters. *IEEE Trans. Ind. Inform.* **2013**, *10*, 991–1002.
54. Zhang, Y.; Xie, W. Low complexity model predictive control-Single vector-based approach. *IEEE Trans. Power Electron.* **2013**, *29*, 5532–5541. [CrossRef]
55. Zhao, W.; Wang, H.; Tao, T.; Xu, D. Model predictive torque control of five-phase PMSM by using double virtual voltage vectors based on geometric principle. *IEEE Trans. Transp. Electrif.* **2021**, *7*, 2635–2644. [CrossRef]
56. Zhang, Y.; Zhang, P.; Fan, H.; Wang, S. An Improved Multi-Vector Model Predictive Torque Control Based on Virtual Voltage Vector. In Proceedings of the 2023 IEEE 6th Student Conference on Electric Machines and Systems (SCEMS), Huzhou, China, 7–9 December 2023; pp. 1–6.
57. Arahal, M.R.; Satué, M.G.; Barrero, F. Multi-phase weighted stator current tracking using a hyper-plane partition of the control set. *Control Eng. Pract.* **2024**, *153*, 106114. [CrossRef]
58. Mamdouh, M.; Abido, M.A. Current Gradient Based Modified Hysteresis Controller for Asymmetrical Six-phase Induction Motor. *IEEE J. Emerg. Sel. Top. Power Electron.* **2024**, *12*, 5164–5175. [CrossRef]
59. Hoffmann, N.; Andresen, M.; Fuchs, F.W.; Asiminoaei, L.; Thogersen, P. Variable sampling time finite control-set model predictive current control for voltage source inverters. In Proceedings of the Energy Conversion Congress and Exposition (ECCE), Raleigh, NC, USA, 15–20 September 2012; pp. 2215–2222.
60. Arahal, M.; Satué, M.; Barrero, F.; Colodro, F. Variable sampling period multi-phase predictive controller based on regions. *Control Eng. Pract.* **2024**, *151*, 106021. [CrossRef]
61. Arahal, M.R.; Barrero, F.; Satué, M.G.; Martín, C.; Bermúdez, M. Evolutionary Gaps Stator Current Control of Multiphase Drives Balancing Harmonic Content. *IEEE Trans. Ind. Electron.* **2024**, *71*, 6886–6893. [CrossRef]
62. Flach, E.; Hoffmann, R.; Mutschler, P. Direct mean torque control of an induction motor. In Proceedings of the European Conference on Power Electronics and Applications, Trondheim, Norway, 8–10 September 1997; Volume 3, pp. 672–677.
63. Wang, H.; Wu, X.; Zheng, X.; Yuan, X. Model Predictive Current Control of Nine-Phase Open-End Winding PMSMs With an Online Virtual Vector Synthesis Strategy. *IEEE Trans. Ind. Electron.* **2022**, *70*, 2199–2208. [CrossRef]
64. Li, T.; Sun, X.; Lei, G.; Yang, Z.; Guo, Y.; Zhu, J. Finite-control-set model predictive control of permanent magnet synchronous motor drive systems—An overview. *IEEE/CAA J. Autom. Sin.* **2022**, *9*, 2087–2105. [CrossRef]

65. Gokdag, M. Modulated Predictive Control to Improve the Steady-State Performance of NSI-Based Electrification Systems. *Energies* **2022**, *15*, 2043. [CrossRef]
66. Aciego, J.J.; González Prieto, I.; Duran, M.J.; Bermudez, M.; Salas-Biedma, P. Model Predictive Control Based on Dynamic Voltage Vectors for Six-Phase Induction Machines. *IEEE J. Emerg. Sel. Top. Power Electron.* **2021**, *9*, 2710–2722. [CrossRef]
67. Luo, Y.; Liu, C. Multi-vector-based model predictive torque control for a six-phase PMSM motor with fixed switching frequency. *IEEE Trans. Energy Convers.* **2019**, *34*, 1369–1379. [CrossRef]
68. Yan, L.; Zhang, X.; Yang, J.; Yang, G.; Deng, R. Synthetic Vectors-Based Predictive Control of Dual Three-Phase PMSMs for Current Harmonics Mitigation Considering Average Deception Effect. *IEEE J. Emerg. Sel. Top. Power Electron.* **2024**, *12*, 3103–3114. [CrossRef]
69. Song, X.; Wang, H.; Ma, X.; Yuan, X.; Wu, X. Robust Model Predictive Current Control for a Nine-Phase Open-End Winding PMSM With High Computational Efficiency. *IEEE Trans. Power Electron.* **2023**, *38*, 13933–13943. [CrossRef]
70. Wang, H.; Zheng, X.; Yuan, X.; Wu, X. Low-Complexity Model-Predictive Control for a Nine-Phase Open-End Winding PMSM With Dead-Time Compensation. *IEEE Trans. Power Electron.* **2022**, *37*, 8895–8908. [CrossRef]
71. Xu, Z.; Wang, Z.; Wang, X.; Cheng, M. Predictive current control method for dual three-phase PMSM drives with reduced switching frequency and low-computation burden. *IET Electr. Power Appl.* **2020**, *14*, 668–677. [CrossRef]
72. Aciego, J.J.; Gonzalez-Prieto, I.; Duran, M.J.; Gonzalez-Prieto, A.; Carrillo-Rios, J. Guiding the Selection of Multi-Vector Model Predictive Control Techniques for Multiphase Drives. *Machines* **2024**, *12*, 115. [CrossRef]
73. Mamdouh, M.; Abido, M.A. Simple predictive current control of asymmetrical six-phase induction motor with improved performance. *IEEE Trans. Ind. Electron.* **2022**, *70*, 7580–7590. [CrossRef]
74. Xue, C.; Song, W.; Wu, X.; Feng, X. A constant switching frequency finite-control-set predictive current control scheme of a five-phase inverter with duty-ratio optimization. *IEEE Trans. Power Electron.* **2017**, *33*, 3583–3594. [CrossRef]
75. Gonzalez-Prieto, I.; Duran, M.J.; Aciego, J.J.; Martin, C.; Barrero, F. Model predictive control of six-phase induction motor drives using virtual voltage vectors. *IEEE Trans. Ind. Electron.* **2017**, *65*, 27–37. [CrossRef]
76. Barrero, F.; Arahal, M.R.; Gregor, R.; Toral, S.; Duran, M.J. A Proof of Concept Study of Predictive Current Control for VSI-Driven Asymmetrical Dual Three-Phase AC Machines. *IEEE Trans. Ind. Electron.* **2009**, *56*, 1937–1954. [CrossRef]
77. Yu, B.; Song, W.; Tang, T.; Wang, S.; Yang, P. A Finite Control Set Model Predictive Current Control Scheme for Five-phase PMSMs Based on Optimized Duty Ratio. In Proceedings of the 2019 IEEE Applied Power Electronics Conference and Exposition (APEC), Anaheim, CA, USA, 17–21 March 2019; pp. 2564–2569. [CrossRef]
78. Gajanan Petkar, S.; Vinay Kumar, T. Computationally efficient model predictive control of three-level open-end winding permanent-magnet synchronous motor drive. *IET Electr. Power Appl.* **2020**, *14*, 1210–1220. [CrossRef]
79. Wang, W.; Liu, C.; Liu, S.; Zhao, H. Model Predictive Torque Control for Dual Three-Phase PMSMs with Simplified Deadbeat Solution and Discrete Space-Vector Modulation. *IEEE Trans. Energy Convers.* **2021**, *36*, 1491–1499. [CrossRef]
80. Wang, W.; Liu, C.; Zhao, H.; Song, Z. Improved Deadbeat-Direct Torque and Flux Control for PMSM With Less Computation and Enhanced Robustness. *IEEE Trans. Ind. Electron.* **2023**, *70*, 2254–2263. [CrossRef]
81. Lin, X.; Huang, W.; Jiang, W.; Zhao, Y.; Zhu, S. Deadbeat Direct Torque and Flux Control for Permanent Magnet Synchronous Motor Based on Stator Flux Oriented. *IEEE Trans. Power Electron.* **2020**, *35*, 5078–5092. [CrossRef]
82. Song, W.; Saeed, M.S.R.; Yu, B.; Li, J.; Guo, Y. Model Predictive Current Control With Reduced Complexity for Five-Phase Three-Level NPC Voltage-Source Inverters. *IEEE Trans. Transp. Electrif.* **2022**, *8*, 1906–1917. [CrossRef]
83. Xiong, C.; Xu, H.; Guan, T.; Zhou, P. A Constant Switching Frequency Multiple-Vector-Based Model Predictive Current Control of Five-Phase PMSM With Nonsinusoidal Back EMF. *IEEE Trans. Ind. Electron.* **2020**, *67*, 1695–1707. [CrossRef]
84. Luo, Y.; Liu, C. Model Predictive Control for a Six-Phase PMSM Motor with a Reduced-Dimension Cost Function. *IEEE Trans. Ind. Electron.* **2020**, *67*, 969–979. [CrossRef]
85. Sun, T.; Jia, C.; Liang, J.; Li, K.; Peng, L.; Wang, Z.; Huang, H. Improved modulated model-predictive control for PMSM drives with reduced computational burden. *IET Power Electron.* **2020**, *13*, 3163–3170. [CrossRef]
86. Luo, Y.; Liu, C. Elimination of Harmonic Currents Using a Reference Voltage Vector Based-Model Predictive Control for a Six-Phase PMSM Motor. *IEEE Trans. Power Electron.* **2019**, *34*, 6960–6972. [CrossRef]
87. Duran, M.J.; Gonzalez-Prieto, I.; Gonzalez-Prieto, A.; Aciego, J.J. The evolution of model predictive control in multiphase electric drives: A growing field of research. *IEEE Ind. Electron. Mag.* **2022**, *16*, 29–39. [CrossRef]
88. Gonçalves, P.F.; Cruz, S.M.; Mendes, A.M. Bi-subspace predictive current control of six-phase PMSM drives based on virtual vectors with optimal amplitude. *IET Electr. Power Appl.* **2019**, *13*, 1672–1683. [CrossRef]
89. He, Y.; Tang, Y.; Chen, Q.; Wang, F.; Kennel, R. Deadbeat Direct Power Control of Voltage-Sourced Rectifier with Reduced Switching Frequency. In Proceedings of the 2020 23rd International Conference on Electrical Machines and Systems (ICEMS), Hamamatsu, Japan, 24–27 November 2020; pp. 1511–1515.
90. Rohten, J.A.; Dewar, D.N.; Zanchetta, P.; Formentini, A.; Munoz, J.A.; Baier, C.R.; Silva, J.J. Multivariable deadbeat control of power electronics converters with fast dynamic response and fixed switching frequency. *Energies* **2021**, *14*, 313. [CrossRef]
91. Yin, R.; Yang, J. Predictive current control for seven-phase induction motor based on the optimal operating time of four-dimensional vector. *IET Electr. Power Appl.* **2019**, *13*, 1684–1695. [CrossRef]
92. Dai, S.; Wang, J.; Sun, Z.; Chong, E. Deadbeat predictive current control for high-speed permanent magnet synchronous machine drives with low switching-to-fundamental frequency ratios. *IEEE Trans. Ind. Electron.* **2021**, *69*, 4510–4521. [CrossRef]

93. Saeed, M.S.; Song, W.; Yu, B.; Wu, X. Low-complexity deadbeat model predictive current control with duty ratio for five-phase PMSM drives. *IEEE Trans. Power Electron.* **2020**, *35*, 12085–12099. [CrossRef]
94. Li, Z.; Zheng, X.; Xia, J.; Wang, L.; Guo, Y.; Gao, X.; Liu, Z.; Zhang, X. Modulated-Virtual-Vector-Based Predictive Current Control for Dual Three-Phase PMSM With Enhanced Steady-State Performance. In Proceedings of the IECON 2023-49th Annual Conference of the IEEE Industrial Electronics Society, Singapore, 16–19 October 2023; pp. 1–6.
95. Zhang, H.; Zhang, Y.; Zhu, Y.; Wang, X. Robust deadbeat predictive current control of induction motor drives with improved steady state performance. *IET Power Electron.* **2023**, *16*, 1281–1292. [CrossRef]
96. Arahal, M.R.; Barrero, F.; Duran, M.J.; Ortega, M.G.; Martin, C. Trade-offs analysis in predictive current control of multi-phase induction machines. *Control Eng. Pract.* **2018**, *81*, 105–113. [CrossRef]
97. Fretes, H.; Rodas, J.; Doval-Gandoy, J.; Gomez, V.; Gomez, N.; Novak, M.; Rodriguez, J.; Dragičević, T. Pareto Optimal Weighting Factor Design of Predictive Current Controller of a Six-Phase Induction Machine based on Particle Swarm Optimization Algorithm. *IEEE J. Emerg. Sel. Top. Power Electron.* **2021**, *10*, 207–219. [CrossRef]
98. Mamdouh, M.; Abido, M.; Hamouz, Z. Weighting Factor Selection Techniques for Predictive Torque Control of Induction Motor Drives: A Comparison Study. *Arab. J. Sci. Eng.* **2018**, *43*, 433–445. [CrossRef]
99. Zhang, Y.; Cao, K.; Yi, W.; Meng, Y.; Cheng, Z. Three-Phase Duty Cycle Modulation-Based Model Predictive Control Strategy for QZSI-PMSM System without Cost Function. *Prog. Electromagn. Res. C* **2024**, *148*, 205–217. [CrossRef]
100. Zhang, Y.; Liu, Y.; Luo, B.; Ling, Y. Variable weight coefficient MPC control strategy for qZSI-VSG wind power grid-connected system. *IET Renew. Power Gener.* **2023**, *17*, 1952–1965. [CrossRef]
101. Guazzelli, P.R.U.; de Andrade Pereira, W.C.; de Oliveira, C.M.R.; de Castro, A.G.; de Aguiar, M.L. Weighting factors optimization of predictive torque control of induction motor by multiobjective genetic algorithm. *IEEE Trans. Power Electron.* **2019**, *34*, 6628–6638. [CrossRef]
102. Arshad, M.H.; Abido, M.A.; Salem, A.; Elsayed, A.H. Weighting factors optimization of model predictive torque control of induction motor using NSGA-II with TOPSIS decision making. *IEEE Access* **2019**, *7*, 177595–177606. [CrossRef]
103. Yao, C.; Sun, Z.; Xu, S.; Zhang, H.; Ren, G.; Ma, G. ANN optimization of weighting factors using genetic algorithm for model predictive control of PMSM drives. *IEEE Trans. Ind. Appl.* **2022**, *58*, 7346–7362. [CrossRef]
104. Arahal, M.R.; Kowal, A.; Barrero, F.; Castilla, M. Cost function optimization for multi-phase induction machines predictive control. *Rev. Iberoam. Autom. Inform. Ind.* **2019**, *16*, 48–55. [CrossRef]
105. Deng, A.; Yang, W.; Hu, G.; Huang, W.; Xu, D. Reinforcement Learning based Weight-Tuning Model Predictive Control of Permanent Magnet Synchronous Motor. In Proceedings of the 2024 IEEE 10th International Power Electronics and Motion Control Conference (IPEMC2024-ECCE Asia), Chengdu, China, 17–20 May 2024; pp. 317–322.
106. Muddineni, V.P.; Sandepudi, S.R.; Bonala, A.K. Finite control set predictive torque control for induction motor drive with simplified weighting factor selection using TOPSIS method. *IET Electr. Power Appl.* **2017**, *11*, 749–760. [CrossRef]
107. Arahal, M.R.; Satué, M.G.; Colodro, F.; Martínez-Heredia, J.M. Trade-Off Analysis of Drive Dynamics Considering Speed and Current Loops. *Energies* **2024**, *17*, 3649. [CrossRef]
108. Ravi Eswar, K.M.; Venkata Praveen Kumar, K.; Vinay Kumar, T. Enhanced predictive torque control with auto-tuning feature for induction motor drive. *Electr. Power Components Syst.* **2018**, *46*, 825–836. [CrossRef]
109. Liu, X.; Qiu, L.; Wu, W.; Ma, J.; Fang, Y.; Peng, Z.; Wang, D. Neural predictor-based low switching frequency FCS-MPC for MMC with online weighting factors tuning. *IEEE Trans. Power Electron.* **2021**, *37*, 4065–4079. [CrossRef]
110. Arahal, M.R.; Satué, M.G.; Martínez-Heredia, J.M. Multi-Phase Stator Current Tracking with Gradual Penalization of Commutations. *Appl. Sci.* **2024**, *14*, 6005. [CrossRef]
111. Satué, M.G.; Barrero, F.; Martínez-Heredia, J.M.; Colodro, F. Concurrent AI Tuning of a Double-Loop Controller for Multi-Phase Drives. *Machines* **2024**, *12*, 899. [CrossRef]

Disclaimer/Publisher's Note: The statements, opinions and data contained in all publications are solely those of the individual author(s) and contributor(s) and not of MDPI and/or the editor(s). MDPI and/or the editor(s) disclaim responsibility for any injury to people or property resulting from any ideas, methods, instructions or products referred to in the content.